Separation of Hydrodynamic, Entropy, and Combustion Noise in a Gas Turbine Combustor

M. Muthukrishnan,* W. C. Strahle,† and D. H. Neale‡
School of Aerospace Engineering, Georgia Institute of Technology, Atlanta, Ga.

This paper deals with noise sources which are central to the problem of core engine noise in turbopropulsion systems. The sources dealt with are entropy noise and direct combustion noise, as well as a nonpropagating psuedosound which is hydrodynamic noise. It is shown analytically and experimentally that a transition can occur from a combustion noise-dominant situation to an entropy noise-dominant case if the contraction of a terminating nozzle to the combustor is high enough. In the combustor tested, entropy noise is the dominant source for propagational noise if the combustor is choked at the exit. It is also speculated that there might be another unexplored noise source interior of the combustor. Analysis techniques include spectral, cross spectral, correlation, and ordinary and partial coherence analysis. Measurements include exterior and interior fluctuating and mean pressures and temperatures.

Introduction

IT has been known for some time that there are at least two probable causes for core noise—entropy or indirect noise and direct combustion noise.[1] Direct combustion noise is caused by a fluid dilatation caused by a fluctuating heat release. Entropy noise is caused by hot (or cold) spots passing through the pressure gradients of the turbine assembly. Both noise sources have the same fundamental cause—heat release fluctuations—but they are formed in a different manner. Entropy noise depends upon the heat release history following a fluid element through the combustor, whereas combustion noise depends on the instantaneous aggregate heat release rate fluctuation. The purpose of this program was to isolate the two suspected causes of core noise and determine their relative importance to the core noise problem.

It is clear that core noise presents a noise floor in current turbopropulsion systems, but there is controversy concerning the strength of core noise relative to other sources.[2-4] It is sufficient to remark here that core noise exists and is measurable. Entropy and combustion noise are not the only possibilities for core noise. Another possibility is vorticity-nozzle interaction nose,[5] which is essentially a resistance of a nozzle to pass an axial velocity fluctuation. While sources other than entropy and combustion noise are not directly investigated here, the analysis techniques do reveal whether or not entropy and combustion noise are dominant over other sources.

The analysis techniques presented essentially try to relate processes taking place inside a combustor to the noise radiated to the surroundings. One troublesome problem encountered in a prior program[6] was the contamination of interior pressure fluctuation measurements by non-propagating psuedosound (hydrodynamic noise). Another purpose of this paper was to eliminate this contaminant as much as possible in order to concentrate on propagational sound and its causes.

Received Sept. 28, 1977; presented as Paper 77-1275 at the AIAA 4th Aeroacoustics Conference, Atlanta, Ga., Oct. 3-5, 1977; revision received Dec. 8, 1977.

Index categories: Noise; Powerplant Design; Airbreathing Propulsion.

*Postdoctoral Fellow. Member AIAA.
†Regents' Professor. Associate Fellow AIAA.
‡Research Engineer. Member AIAA.

Theory

The theory developed in Ref. 6 for a gas turbine unit exhausting directly into the atmosphere did not contain entropy noise explicitly, because hot spots will only generate noise if a pressure gradient is imposed on the exhaust gases. Nevertheless, the theory can be easily modified to account for an exhaust nozzle by modifying the boundary condition at the nozzle end. The theory follows the linearized vorticity-acoustic field equation approach.[7] The theory is presented in detail in Ref. 8 and will only be outlined here.

Dilatation (acoustic) waves are generated by a dilatation of the flow by heat-release fluctuations (combustion noise) and by hot spots encountering the nozzle (entropy noise). The boundary conditions employed are: a) a right circular combustor with a hard-head end b) a side wall characterized by a specific acoustic admittance, β_w, and an exit plane characterized by the two admittance coefficients β_e and α corresponding to the isentropic and entropy admittance coefficients, respectively.[9] An eigenfunction expansion and numerical computation shows that only the plane-wave mode need to be considered in the frequency range of interest (≤ 1000 Hz),[6] which considerably simplifies the problem.

In terms of dimensionless variables, the solution for the Fourier transform of the acoustic pressure at a point downstream of the combustion zone may be written as

$$\hat{p}_\omega(x) = f_1(\omega; \text{problem parameters}) \int_V Q_\omega \cos k_{oo} x \, dV + f_2(\omega; \text{problem parameters})\, \sigma_{\omega_e} \tag{1}$$

In Eq. (1), f_1 and f_2 are dimensionless, calculable transfer functions, x is axial position, V is the combustor volume, and k_{oo} is the wave number where the quantities are made dimensionless by using the combustor length as the reference length scale. The reference pressure is the steady-state combustor pressure; Q_ω is the Fourier transform of the dimensionless heat-release fluctuation; and σ_{ω_e} is the Fourier transform of the cross section average of the relative temperature fluctuations at the nozzle entrance plane. $f_2 \propto \alpha$ and $\alpha = 0$ for no nozzle, such that Eq. (1) reduces to the theory of Ref. 6 for the case of no nozzle. In the actual measurements, $\hat{p}_\omega$ is not the only pressure sensed at a microphone, but there is hydrodynamic noise contamination. The true measured pressure transform is p_ω given by

$$p_\omega = \hat{p}_\omega + H_\omega$$

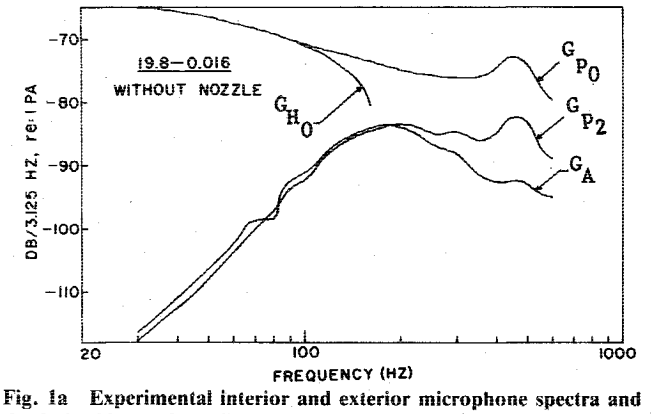

Fig. 1a Experimental interior and exterior microphone spectra and the derived heat release fluctuation and hydrodynamic noise spectra.

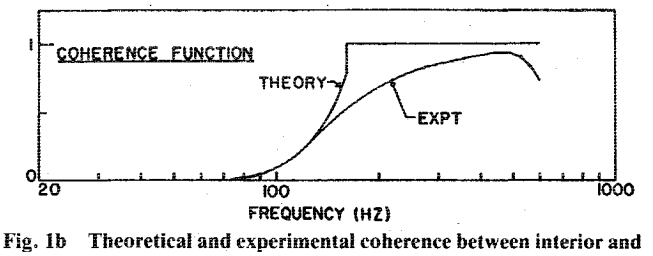

Fig. 1b Theoretical and experimental coherence between interior and near-field microphones.

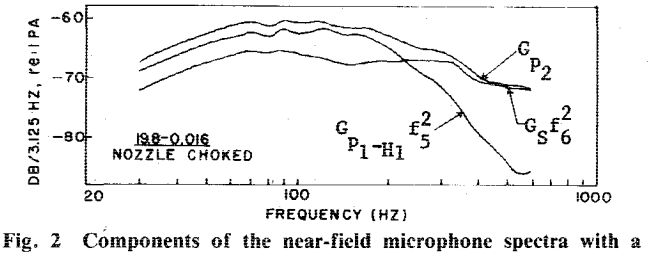

Fig. 2 Components of the near-field microphone spectra with a choked nozzle.

where H_ω is the transform of the hydrodynamic noise component and is assumed incoherent with $\hat{p}_\omega$.

Now let the one-sided spectral densities be formed from the Fourier transforms[10] and be called G_p, G_H, G_S and G_A for the pressure, hydrodynamic noise, σ_{ω_e} components, and volume integral of Eq. (1), respectively. Let location 0 be an interior measurement at position x, location 1 be the nozzle entrance plane, and location 2 be the nozzle exit plane. Then

$$G_{p_0} = G_A f_1^2 + G_S f_2^2 + G_{H_0}$$

$$G_{p_1} = G_A f_3^2 + G_S f_4^2 + G_{H_1}$$

$$G_{p_2} = G_{p_1 - H_1} f_5^2 + G_S f_6^2 \qquad (2)$$

The f_i are all computable transform functions and are given in Ref. 8. It has been experimentally verified that if the p_2 microphone is placed just outside the exhaust stream, the hydrodynamic noise is overwhelmed by propagational sound; hence, no hydrodynamic noise term is included in G_{p_1}. Moreover, only the part of p_1 that is propagational contributes to p_2, so that $G_{p_1-H_1} = G_{p_1} - G_{H_1}$ is the convention used in Eq. (2).

Shown in Figs. 1a and 1b are the results of some calculations made with Eqs. (2) for the no-nozzle case, using data from Ref. 6. G_{p_2} is an experimental curve. Since $f_2 = f_4 = f_6 = 0$ in this case, G_A is calculable from Eqs. (2). Actually, an unknown in this calculation is the value of the combustor liner acoustic admittance, and this number is chosen so that the theoretical curve best osculates the 400 Hz quarter-wave resonance peak on Fig. 1a. The calculated G_A is shown on Fig. 1a. Then G_{H_0} is calculable from Eqs. (2) and is shown on Fig. 1a. When G_{p_0} and G_{H_0} become separated more than about 6 dB, the calculation is subject to high error so that G_{H_0} is arbitrarily set to zero. In this calculation, the hydrodynamic noise becomes negligible compared with the combustion noise above about 130 Hz. As a check, the coherence function between the interior and exterior microphone is computed with G_{H_0} as the only contaminant to the measurement. This is compared experimentally in Fig. 1b with a satisfactory agreement.

Next, assuming that G_{H_0} and G_A are unaltered, a case with a choked nozzle is considered. Calculations of G_S are taken from the experimental results of the next section. The calculations are shown in Fig. 2. The components of G_{p_2} due to entropy and the entrance plane pressure are shown. The major point is that above about 200 Hz, entropy noise dominates the noise output. Although not shown, combustion noise still dominates p_0 and p_1, showing that the generation of transmitted pressure waves by the hot spots is the dominant noise generation process in the choked nozzle case.

The major point is that for fixed combustor mass flow and air/fuel ratio, a transition from a combustion noise to an entropy noise situation may be expected, as the terminating nozzle contraction ratio increases toward a choking condition. The next section will show experimentally that this is, in fact, observed.

Under appropriate simplifications, it is shown in Ref. 8 that the dimensionless entropy flunctuation at the nozzle entrance plane is given by

$$\sigma_{\omega_e} = g(\omega) \int_V \exp\left[i\omega \int_0^{x'} \frac{dx'}{\bar{u}} \right] \frac{Q_\omega}{\bar{u}} dV \qquad (3)$$

Equation (3) is compared with Eq. (1) to see if there is a coherent relationship between the combustion noise term and the entropy noise term. Equation (3) clearly shows how the entropy is developed while following a fluid element along its path [$(\int_0^x dx'/\bar{u}(x')$ is a fluid travel time]. Here $\bar{u}$ is the average one-dimensional axial gas velocity divided by the exit plane speed of sound. In the limit of very low frequency, so that the exponential terms in Eq. (3) and $\cos k_{oo} x$ in Eq. (1) $\rightarrow 1$, it is clearly seen that the heat-release fluctuation terms are almost identical. That is, there would be a high coherence between combustion and entropy noise, so that it would be meaningless to attempt to separate them. On the other hand, at only moderate frequencies, the exponentials in Eq. (3) become rapidly oscillatory in phase. This has the effect of destroying the coherence between the two noise source terms and, in effect, makes them independent, uncorrelated sources.

The transition between coherence and incoherence should take place roughly where $\omega/\bar{u}_c \approx 1$ or at a frequency which is the inverse of a particle stay-time in the combustor. For the combustor used in this program, this frequency is of the order of 100 Hz. Consequently, above this frequency it is reasonable to assume that the combustion and entropy noise sources are uncorrelated. Evidence that the two sources are highly correlated at low frequency is presented in the experimental portion of this paper.

Experimental Apparatus

The acoustic experiments, explained in the following sections, have been carried out on a combustor taken from a Boeing 502-7D gas turbine unit. Some initial results, concerning combustion noise radiation characteristics and coherence estimates between interior and exterior measurements for the Boeing combustor, have been reported in Ref. 6, where the hot exhaust gases were discharged directly into atmosphere at very low exit Mach numbers without encountering any strong pressure gradient. As stated earlier, the presence of a strong mean pressure gradient is one of the requisites for entropy noise generation and, in the present

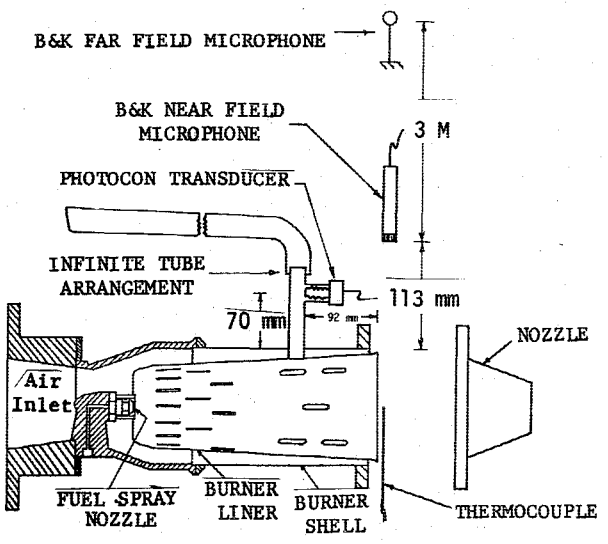

Fig. 3 Schematic of experimental setup.

program, such a pressure gradient is imposed on the hot gases by attaching to the burner exit a convergent nozzle of 3:1 area reduction or an orfice plate with 9 holes of 14-mm diam each and having an effective area reduction of 10.5:1. An exit Mach number, $M_2 = 0.20$, is obtained with this nozzle; whereas, at high Mach numbers, $M_2 = 0.6$, 0.8, and 1.0, the jet is exhausted through a multihole orifice plate rather than a single opening nozzle in order to keep the jet noise interference low. A case of low exit Mach number, $M_2 = 0.05$, obtained by direct discharge into the atmosphere without any end attachment, is also included for the purpose of comparison. The experimental setup with the relative locations of the transducers is shown in Fig. 3. The details of the combustor geometry and its operating characteristics are explained in Refs. 8 and 11. The pressure fluctuations inside the combustor and the near-field and far-field radiated sound pressures have been measured through a photocon pressure transducer and Brüel and Kjaer type 4134, 12-mm condenser microphones, respectively. The location of the photocon pressure transducer, displaced from the flowfield, is expected to keep the contamination by nonpropagational hydrodynamic noise to a minimum. Since it is feared that, at high Mach numbers, the far-field measurements may be contaminated by jet noise, a near-field microphone is also included for the purpose of spectral comparisons and coherence estimates between interior and exterior noise measurements. This near-field microphone, by virtue of its location, may be expected to receive a greater relative proportion of core than jet noise than the far-field microphone. This is confirmed in later sections. Moreover, it was established in a previous investigation (Ref. 6) that the near-field measurements were free from ground reflection effects which mask the far-field spectra. Since the entropy noise study requires the details of the combustion-generated hot spots, a measurement program has been carried out to obtain the temperature fluctuation characteristics. Fast response chromel-alumel thermocouples of 0.025 mm wire diam are used to record the temperature fluctuations at the burner exit plane, as shown in Fig. 3. A novel method to determine the time constants of the thermocouples has been developed during the course of this program and is fully explained in Ref. 12. Unlike the conventional method of providing electrical compensation networks, the thermocouple signals, in the present program, have been compensated for these time constants later during data analysis by suitable modification of the Fourier analyzer programming. All the signals, after amplification, are recorded on a FM tape for later signal analysis. The recorded signals have been analyzed for spectral content and coherence estimates through a Fourier analyzer system.

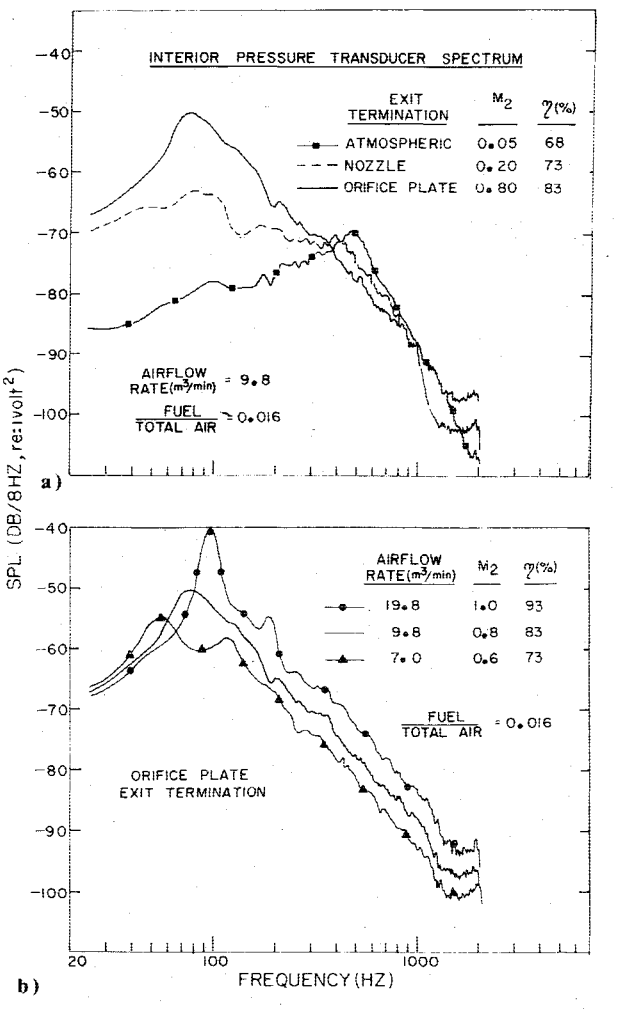

Fig. 4 Interior pressure transducer spectra as a function of airflow rate and overall fuel/air ratio.

Results and Discussion

Spectral Characteristics

Figure 4 shows the spectral of interior pressure fluctuations. The upper frequency limit is chosen as 2000 Hz, because the information of interest falls below this limit. An exit Mach number $M_2 = 0.05$ represents a burner can operating without a nozzle, while $M_2 = 0.20$ belongs to the convergent nozzle case and $M_2 = 0.6$, 0.8, and 1.0 come through the use of orifice plate. The airflow rates vary between 7.0 and 19.8 m^3/min. The overall fuel/air ratio is maintained constant at 0.016 for all cases. Out of a wide range of test runs, only the preceding conditions are selected for the purpose of comparison of results. Figure 4a illustrates the spectral changes with increasing pressure drop across the combustor as the exit termination is changed for a fixed airflow rate and fuel/air ratio; whereas Fig. 4b shows the spectral behavior with the increasing pressure drop across the orifice plate for varying airflow rates and a fixed fuel/air ratio. It can be seen from Fig. 4a that, as the exit contraction ratio is increased, the spectral level rises significantly with an increase in the exit Mach number in the lower frequency range of 0-300 Hz. Around 300 Hz, all attain almost the same level, and then they fall off rapidly at the same rate (10 dB/octave) with increasing frequency. Another observation made here is that the interior spectrum corresponding to the exit Mach number, $M_2 = 0.05$, exhibits a quarter-wave resonance peak around 500 Hz. With an increase in the exit contraction ratio corresponding to high Mach number cases, this resonance peak should shift to a higher frequency range (800-1000 Hz), tending toward a half-wave resonance. On the contrary, these peaks have disappeared in the high Mach number cases. Such

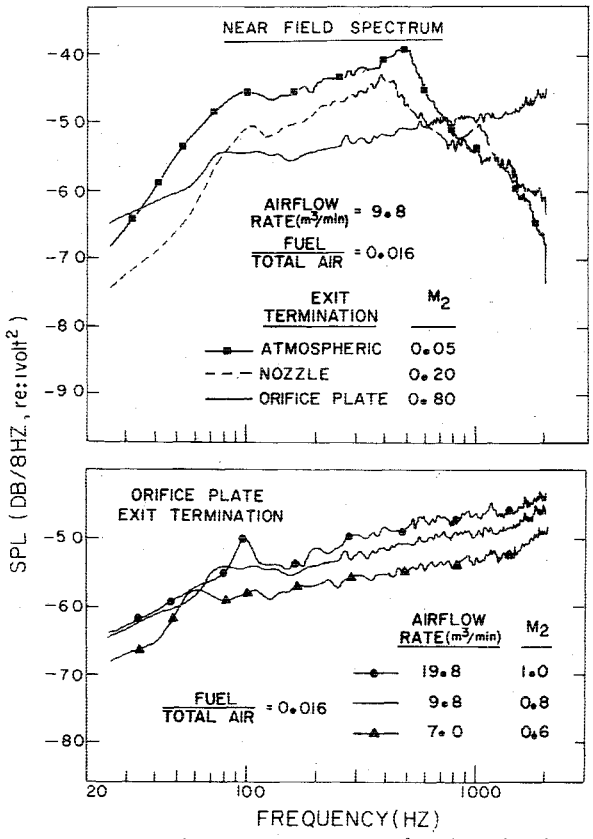

Fig. 5 Near-field microphone spectra as a function of airflow rate and overall fuel/air ratio.

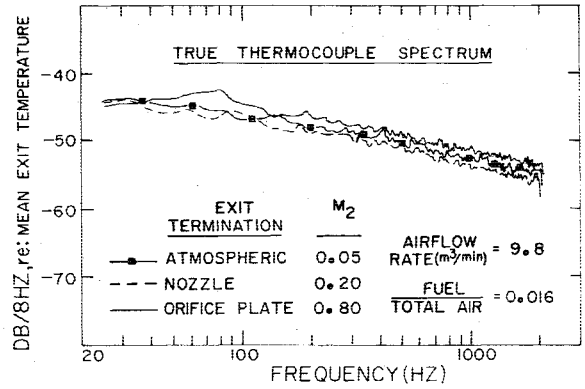

Fig. 6 Temperature fluctuation spectra for a few typical operating conditions.

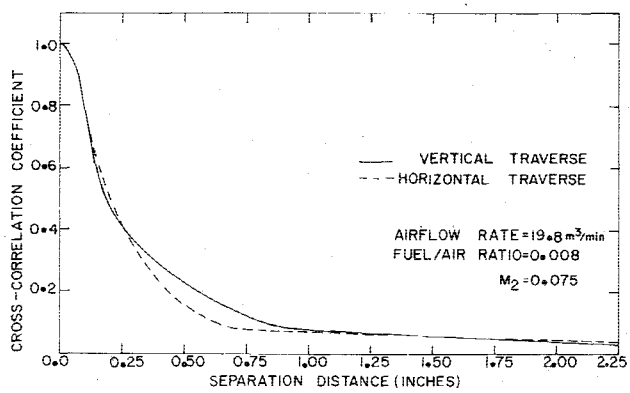

Fig. 7 Cross correlation coefficients as a function of separation distance between two thermocouples for different traverse directions.

peaks have been seen in experiments, not reported here, when using a flush-mounted interior transducer. The occurrence of a peak around 100 Hz in the case of high Mach numbers is explained at the end of this section.

Figure 5 shows the near-field spectra for the same run conditions. At low exit Mach numbers, the familiar combustion noise hump occurs around 200 Hz with burner can resonances superimposed around 500 Hz, depending on the type of exit termination. But the near-field spectra pertaining to high Mach number cases do not exhibit the usual combustion noise characteristics. The change in the spectral shapes at high Mach numbers could mean either entropy noise domination or jet noise contamination of the near-field signal. Although the sound pressure levels of jet noise were slightly higher than core noise levels at higher exit Mach numbers, a comparison of near-field spectra belonging to a hot case and a cold one of identical exit velocities (Ref. 8) reveals that the hot spectrum is consistently at a lower level (about 3 dB) than the cold one, at least in the range of 150 to 1000 Hz. This fact, coupled with the scaling laws for sound power levels obtained through the near-field microphone data, confirm the dominance of core noise over jet noise, at least in the frequency range of interest (150-1000 Hz). Later in this section, it is shown through coherence estimates that it is indeed the entropy noise that contributes significantly to the near-field signal at high exit Mach numbers.

Typical spectra of the temperature fluctuations at the burner exit plane are shown in Fig. 6. The spectral shapes of the temperature fluctuations corresponding to different exit terminations, as seen from Fig. 6, are found to be very similar. The temperature fluctuation spectrum is a broadband one and low frequency in nature. The spectrum gradually falls off with an increase in frequency. The rms temperature fluctuations are found to vary within a range of 9 to 14% of the mean temperature for various cases.

The theoretical evaluation of entropy noise requires a knowledge of the spatial correlation length scales of the temperature fluctuations. Two thermocouples of the same size (0.025 mm wire diam) have been used for this correlation study. One of the thermocouples monitors the temperature fluctuations at a fixed place at the burner exit plane, while the other one registers the signals at various locations, moving radially away from the former. The fixed and the moving thermocouple signals have been cross correlated and normalized to obtain the cross correlation coefficients. The cross correlation coefficient, as a function of the separation distance between the two thermocouples, is shown in Fig. 7 for two cases corresponding to the thermocouple traverses along two different radial directions. In both cases, the temperature fluctuations seem to be correlated over a distance of about 12 mm at the burner exit plane, thereby suggesting a temperature eddy of about 12 mm in size. The constancy of the correlation length scales in various radial directions demonstrates the axisymmetric nature of the thermal eddies. Also, a good similarity in the correlation analysis results is found for two different test conditions (Ref. 8). In all these cases, the cross correlation is found to be positive everywhere with a long tail.

It is important to note that the spectral characteristics of the temperature fluctuations previously mentioned were obtained through single-point thermocouple measurements at the burner exit plane. However, the entropy noise calculations require the quantities averaged over the burner exit area. The conversion from single-point thermocouple measurements to area-averaged quantities requires a knowledge of the correlation area of temperature fluctuations at the burner exit plane. The details of computing this correlation area as a function of frequency is explained in Ref. 8. The variation of the normalized correlation area with the frequency, as obtained by a single radial thermocouple traverse, is shown in Fig. 8. For reasons to be explained later, an average correlation area is also computed from three correlation areas

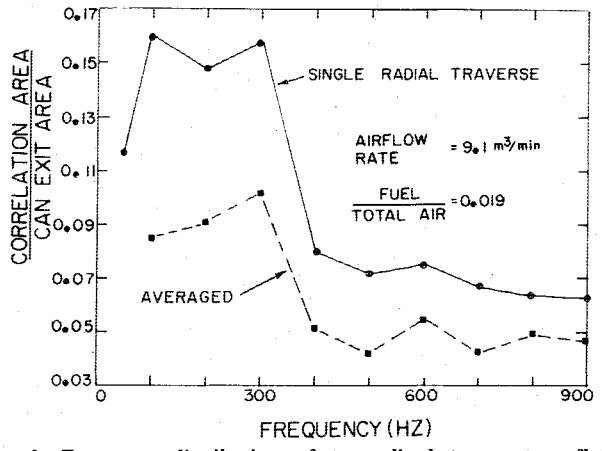

Fig. 8 Frequency distribution of normalized temperature fluctuations correlation area.

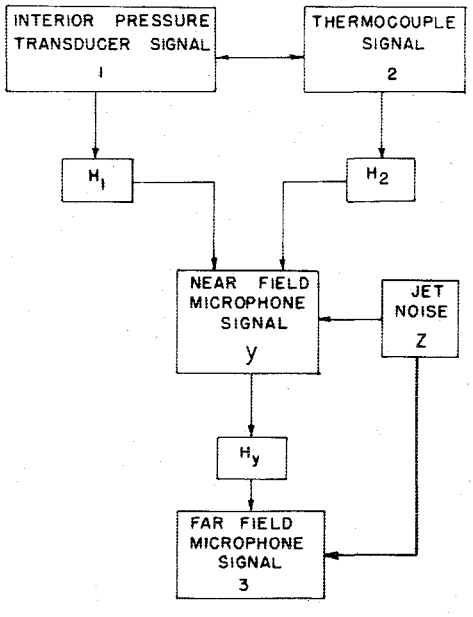

H_1, H_2, H_y TRANSFER FUNCTIONS OF 1, 2, y

Fig. 9 Noise sources model for coherence estimates.

obtained through radial, as well as circumferential thermocouple cross correlations without any end attachment and radial cross correlations with the orifice plate attached. The airflow rate and fuel/air ratio were kept constant at 9.1 m^3/min and 0.019, respectively, in the preceding three test runs. This average temperature correlation area is also shown in Fig. 8. It can be seen from Fig. 8 that the low-frequency temperature fluctuations are correlated over a larger area compared to the high-frequency fluctuations, as is reasonable. Since the correlation area is a measure of the eddy size, it can be said that an eddy representing the low-frequency fluctuations is larger in size compared to that of a high-frequency one.

Coherence Estimates

So far, the spectral characteristics of the individual signals have been discussed in detail. It will be expedient at this stage to look at the coherence between the various signals. Coherence estimates between two signals will bring out the true linear relationship between them.[10] It has a value between 0 and 1. A value of 1 means that the two signals are related by a linear transform operation, regardless of the transform operation. It will be zero if there is no casual relationship between two. Coherence analysis among the

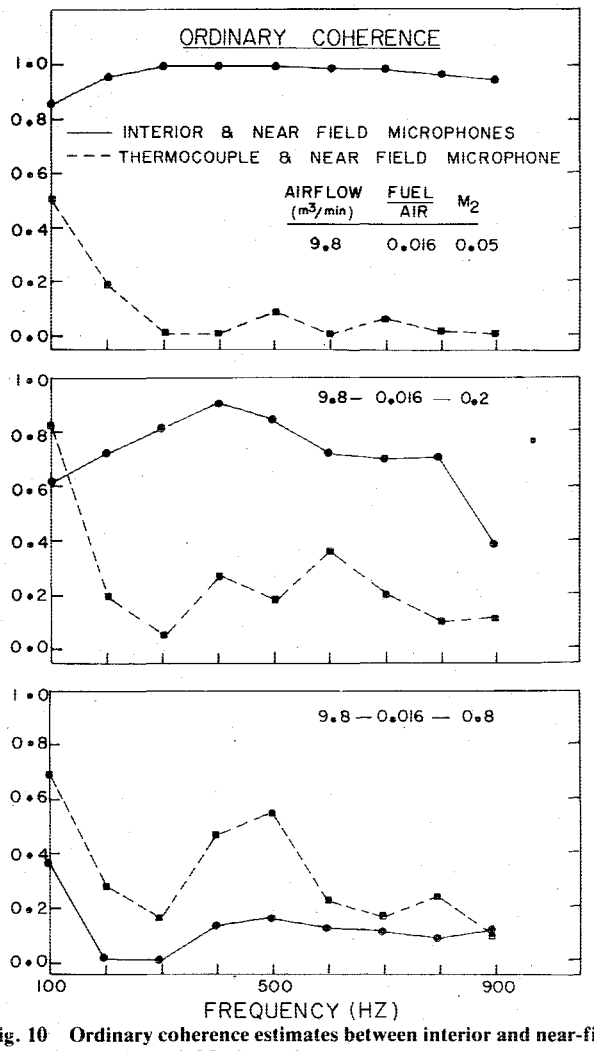

Fig. 10 Ordinary coherence estimates between interior and near-field signals for varying exit Mach numbers.

interior, near- and far-field signals is explained below. Various noise sources and their associated transmission paths are illustrated in Fig. 9. The near-field signal is expected to contain contributions from the two interior sources, namely, combustion and entropy noise sources, as well as from the exterior jet noise. Hence, the coherence between the interior and near-field signals has to be evaluated on the basis of a multiple input problem. In such cases, the degree of linear relationship between any single cause and the effect is best revealed through the partial coherence function analysis which cancels out the effects of other extraneous inputs. The theory of partial coherence functions and the procedures for evaluating them are described in detail in Ref. 10.

The results of the coherence estimates between the interior and the near-field signals are shown in Figs. 10 and 11. It is important to note that the interior sources, namely, the interior pressure transducer and the thermocouple signals, may or may not be correlated. In either case, the coherence analysis takes care of the situation, except that in the uncorrelated case, the expressions become simpler. Reference 8 contains supporting analytical expressions to facilitate the interpretation of these experimental coherence results. Also, the above reference includes results belonging to many test conditions. Because of space limitations, only typical results and their physical significance are given below. Returning to the coherence results, it can be seen from Fig. 10 that the ordinary coherence function level between the interior and near-field microphones generally decreases with an increase in the exit Mach number, while that between the thermocouple and the near-field microphone increases. This result, in-

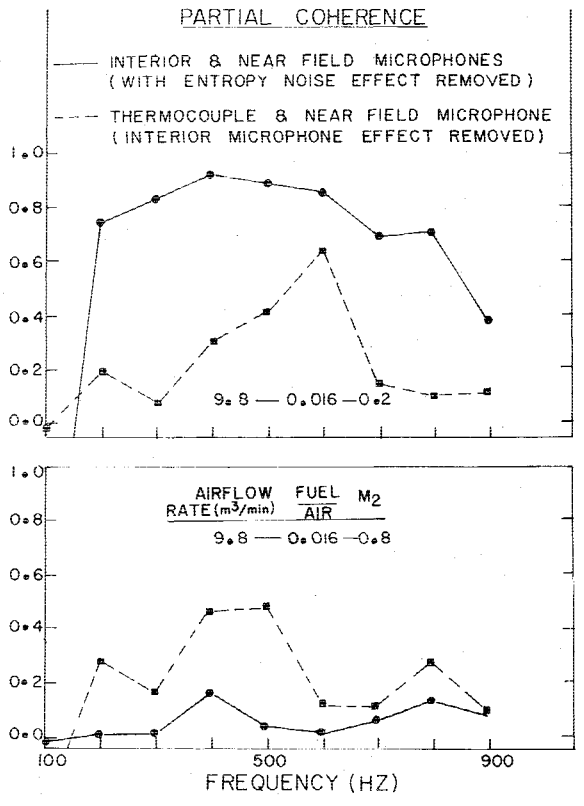

Fig. 11 Partial coherence estimates between interior and near-field signals for varying exit Mach numbers.

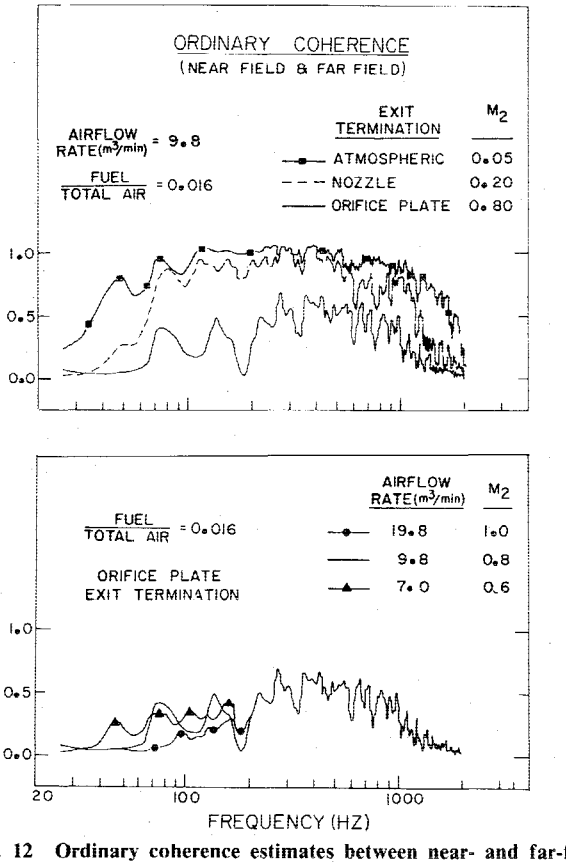

Fig. 12 Ordinary coherence estimates between near- and far-field microphones for different operating conditions.

terpreted in detail in Ref. 8, suggests that the entropy noise contribution available to the near-field microphone starts dominating the combustion contribution available to the near-field microphone signal, with the increase in the exit Mach number. Stated otherwise, there is a gradual transition from a combustion noise-dominated situation at low Mach numbers to an entropy noise-dominated one at high Mach numbers. It is to be noted that this conclusion remains valid, although the presence of a nozzle or orifice plate changes the transmission characteristics of combustion noise.

Partial coherence estimates, another highly useful procedure for the multiple-input problem, also confirm the results in Fig. 11. It can be seen from the figure that with the increase in the exit Mach number, the partial coherence estimate obtained between the thermocouple and the near-field signals, with the interior microphone effects removed, rises above the partial coherence levels evaluated between the interior and the near-field microphone signals, with the effect of the entropy noise removed. This partial coherence result, with the help of Refs. 8 and 10, reestablishes the previous result that the entropy noise starts dominating the near-field signal with the increase in the exit Mach number. In other words, the partial coherence analysis also reaffirms the results of the ordinary coherence function analysis that a combustion noise domination of the near-field signal at low Mach numbers yields to an entropy noise domination at high Mach numbers. It is important to note that in all these partial coherence calculations, the single-point thermocouple measurements were converted into area-averaged quantities using expressions (Ref. 8) which involve the correlation area. A look at Fig. 8 reveals a 2:1 change in the correlation area values computed in two different ways. The coherence results previously discussed are based on the correlation area obtained from a single radial traverse of the thermocouple at the burner exit plane without any nozzle or orifice plate attachment. It is informative to see how sensitive the coherence estimates are to the correlation area values. A detailed analysis in this connection is available in Ref. 8. From the results reported in this reference, it can be said that a decrease in the correlation area values generally increases the partial coherence estimates, with the effect being felt more on the coherence between the thermocouple and the near-field signals than on the one between the interior and the near-field microphones. These arguments lead to the fact that a sufficiently accurate determination of the temperature correlation area distribution is vital for a reliable estimation of the partial coherence. This may be achieved by using a large number of thermocouples at the burner exit plane, so as to obtain more details about the spatial distribution of the temperature fluctuations. The extraordinarily high coherence at about 100 Hz in the case of high Mach numbers is explained at the end of this section. It is important to note that the coherence values in some cases, even after ensemble averaging, are found to be in the range of the statistical errors associated with the coherence estimates. With a view to increasing the reliability of the results, a spectral smoothing technique has been employed in which the spectral estimates corresponding to nine adjacent frequency bands have been averaged. This process reduces the frequency resolution but improves the statistical stability.

The results of the ordinary coherence estimates between the near- and far-field microphones are presented in Fig. 12. A good coherence level exists at low exit Mach numbers. This is attributable to the fact that at these low Mach numbers, the combustion noise contribution to the exterior radiated sound is very high, and, further, its low-frequency nature yields to a monopole radiation pattern. However, at high exit Mach numbers, the coherence level starts decreasing as shown in Fig. 12. This may be due to the fact that with the increasing exit Mach number, the jet noise starts contaminating the core noise radiation. The far-field microphone signal is contaminated to a greater degree than that of near-field, as the former receives the effect of whole jet. However, the near-field microphone receives a greater contribution from core noise radiation with a lesser degree of contamination by jet

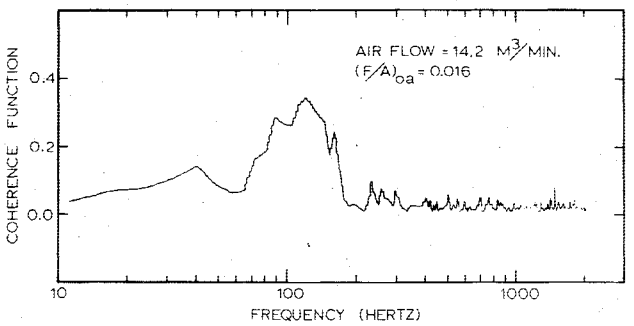

Fig. 13 Coherence between combustion and entropy noise.

noise. This leads to low coherence levels between near- and far-field signals at high exit Mach numbers.

It can be seen from the coherence results of Fig. 10 that in the high Mach number cases, the coherence suddenly jumps to a high value in the vicinity of 100 Hz. The interior and the near-field microphone spectra, as well as the thermocouple spectra, exhibit a similar behavior at the corresponding frequencies, as shown in Fig. 4-6. Many possibilities for the occurrence of this low-frequency peak have been investigated. A speculation about the contribution by the burner stand or the probe to this peak has to be discounted because this occurs only in the high Mach number cases, and, moreover, the corresponding cold flow tests do not exhibit this trend. A suspicion on a longitudinal acoustic resonance phenomenon is ruled out, because the resonant frequency of the combustor, calculated from the speed of sound within the burner rig and the length of the combustor, falls in the range of 400-800 Hz, depending on the nature of the exit termination as supported experimentally by Fig. 4. A strong possibility is that there may be an acoustic coupling between the interior pressure waves and the fuel/air ratio. Pressure waves traveling toward the head end of the burner will bring out a change in the density of the air which causes a change in the fuel/air ratio. This changes the temperature of the fluid traveling toward the nozzle. The temperature change encountering the nozzle in turn produces a new set of pressure waves, augmenting the old set. It is believed that this acoustic feedback is mainly responsible for the observed low-frequency (about 100 Hz) peak, since the frequency of the phenomenon should be governed by the flow speed and the burner length. Calculations show that this frequency falls in the range of 100-200 Hz. This peak, while interesting, is not too significant as far as the overall sound output is concerned in these experiments.

Another result worth mentioning is the coherence between combustion and entropy noise. Figure 13 shows the coherence estimate for a nozzle-off case between a point temperature measurement and the interior wall pressure fluctuation. Note that a point measurement is expected to yield a low coherence, as explained earlier. It can be seen from Fig. 13 that a good coherence exists between combustion and entropy noise around 100 Hz. The poor coherence at very low frequencies is believed to be due to hydrodynamic noise contamination of the interior pressure measurements. The incoherence above 200 Hz suggests a statistical independence of combustion and entropy noise. This transition frequency depends on the flow speed and burner size. These results lend support to the analytical arguments advanced earlier.

It is shown in Ref. 8 from analytical consideration that in the absence of jet noise, the partial coherence function should be unity if there are no intervening noise sources other than combustion and entropy noise. A partial coherence of unity was not achieved with either partial coherence function for either area correlation curve. Moreover, this was not even achieved for runs where the jet noise contamination was low. One could possibly conclude, therefore, that there are some unconsidered noise sources which are important to the core noise problem. Unfortunately, the partial coherence function is relatively sensitive to the correlation area measurements so that this conclusion appears weak. On the other hand, the partial coherence function between the interior and near-field microphones should not suffer from errors in the correlation area, and at high-exit Mach number there is indeed low partial coherence between these two microphones. There is the suspicion, therefore, that at least one other noise source is present which was not investigated in this program. The most likely candidate appears to be vorticity-nozzle interaction noise, which deserves investigation in a future program.

Conclusions

It is to be mentioned that some of the experimental conclusions presented may depend on the apparatus and conditions investigated, such as 1) operation at 2 atm or below, 2) use of a combustor with temperature fluctuations of about 12% of the mean absolute temperature, and 3) length scales of temperature fluctuations of about 1 cm. The important finding of this investigation, supported by both analytical and experimental results, is that at low-exit Mach numbers the exterior radiated sound is mostly attributable to interior combustion noise sources, whereas at high Mach numbers, entropy noise overtakes and dominates combustion-generated noise. Entropy noise domination results because of a combination of a high level of temperature fluctuations existing at the nozzle entrance plane and large pressure gradients being imposed on them. Based on this result, one can conclude that, in the case of actual engines operating generally at choked conditions, entropy noise may be the prime contributor to core engine noise.

Hydrodynamic noise, which is nonpropagational pseudosound, dominates combustion noise in the interior of a combustor below 150 Hz, as revealed by flush-mounted interior pressure transducer measurements (Ref. 6). This fact is supported analytically in this investigation. However, in the present experimental investigation, the contamination of interior pressure measurements by hydrodynamic noise has been confined to the very low-frequency range, 0-50 Hz by locating the pressure transducer at a position displaced from flowfield. It is also shown from analytical and experimental results that combustion and entropy noise are highly correlated, at least in the low-frequency range of 0-100 Hz, thereby making attempts at their separation meaningless.

The nonattainment of unity for the partial coherence results of this investigation, even in the case of low jet noise contamination, leads to a strong belief that some other unexplored propagational noise sources exist. Future work is needed to investigate whether or not vorticity-nozzle interaction noise is involved. The significant differences, observed in the spatial correlation results of temperature fluctuations, demand that in future work, to achieve a good degree of accuracy, a net of thermocouples be used instead of only two thermocouple traverses used in the present investigation.

Acknowledgments

This work was supported by the National Aeronautics and Space Administration under Grant No. NSG 3015 with R. G. Huff as Technical Monitor.

References

[1] Strahle, W. C., "A Review of Combustion Generated Noise," AIAA *Progress in Astronautics and Aeronautics—Aeroacoustics: Jet and Combustion Noise; Duct Acoustics*, Vol. 37, edited by H. T. Nagamatsu, New York, 1975, pp. 229-248.

[2] Mathews, D. G., Rekos Jr., N. F., and Nagel, R. T., "Combustion Noise Investigation," FAA RD-77-3, Feb. 1977.

[3] Stone, J. R., "On the Effects of Flight on Jet Engine Exhaust Noise," NASA TMX-71819, Nov. 1975.

[4] Reshotko, M., "Core Engine Noise Measurement on a YF-102 Engine," AIAA Paper 77-21, 1977.

[5]Pickett, G. F., "Core Engine Noise Due to Temperature Fluctuations Convecting through Turbine Blade Rows," AIAA Paper 75-528, March 1975; also AIAA *Progress in Astronautics and Aeronautics—Aeroacoustics: Jet Noise, Combustion and Core Engine Noise*, Vol. 43, edited by I. R. Schwartz, New York, 1976, pp. 589-608.

[6]Strahle, W. C., Muthukrishnan, M., and Neale, D. H., "Coherence between Internal and External Noise Generated by Gas Turbine Combustors," AIAA Paper 77-20, Jan. 1977; also *AIAA Journal*, Vol. 15, July 1977, pp. 1018-1024.

[7]Goldstein, M. E., *Aeroacoustics*, McGraw-Hill International Book Co., New York, 1976.

[8]Strahle, W. C., Muthukrishnan, M., Neale, D. H., and Ramachandra, M. K., "A Investigation of Combustion and Entropy Noise," NASA CR 135220, July 1977.

[9]Crocco, L. and Sirignano, W. A., "Behavior of Supercritical Nozzles under Three-Dimensional Oscillatory Conditions," AGARDograph No. 117, NATO, 1967.

[10]Bendat, J. S. and Piersol, A. G., *Random Data: Analysis and Measurement Techniques*, Wiley-Interscience, New York, 1971.

[11]Strahle, W. C. and Shivashankara, B. N., "Combustion Generated Noise in Gas Turbine Combustors," NASA CR-134843, Aug. 1974.

[12]Strahle, W. C. and Muthukrishnan, M., "Thermocouple Time Constant Measurements by Cross Power Spectra," *AIAA Journal*, Vol. 14, Nov. 1976, pp. 1642-1644.